agronomy

MDPI

Article

Synthesis of Benzoxazinones Sulphur Analogs and Their Application as Bioherbicides: 1.4-Benzothiazinones and 1.4-Benzoxathianones for Weed Control

Francisco J. R. Mejías [1,2,*], Stefan Schwaiger [2], Rosa M. Varela [1], José M. G. Molinillo [1], Nuria Chinchilla [1,*] and Francisco A. Macías [1]

[1] Allelopathy Group, Department of Organic Chemistry, Institute of Biomolecules (INBIO), Campus de Excelencia Internacional (ceiA3), School of Science, University of Cadiz, 11510 Puerto Real, Spain; rosa.varela@uca.es (R.M.V.); chema.gonzalez@uca.es (J.M.G.M.); famacias@uca.es (F.A.M.)

[2] Institute of Pharmacy, Center for Molecular Biosciences Innsbruck (CMBI), University of Innsbruck, 6020 Innsbruck, Austria; stefan.schwaiger@uibk.ac.at

* Correspondence: javi.rodriguezmejias@uca.es (F.J.R.M.); nuria.chinchilla@uca.es (N.C.)

Abstract: Eight different compounds inspired by benzoxazinones were synthesized in one simple step with easy purification. These compounds have a sulfur atom instead of the oxygen atom present in benzoxazinones. Furthermore, a new derivative obtained by a Rutkauskas–Beresnevicius reaction was synthesized. These compounds were evaluated in vitro to assess their phytotoxicity in plant cells by the elongation of wheat coleoptiles. The novel compounds showed higher inhibition than benzoxazinones and the positive control, especially at higher concentrations (1000 and 300 μM). Benzoxazinones have been described as histidine deacetylase inhibitors and we therefore evaluated the effect of 1.4-benzothiazinones and 1.4-benzoxathianones against HDA6, one of the most important enzymes of the family, in silico by molecular docking and molecular dynamics. In vitro studies against *Echinochloa crus-galli*, *Lolium rigidum* and *Portulaca oleracea* weeds gave interesting results against the growth of the roots for both monocots and dicots. Specifically, the inhibition was more pronounced against dicots, as in the case of common purslane, whose inhibition at a concentration of 1000 μM was similar to that of the classical herbicide employed as a positive control. Higher inhibition was obtained when an aliphatic group was present in the C2 position of 1.4-benzothiazinones.

Keywords: benzothiazinones; bioassay; weeds; allelopathy; docking

Citation: Mejías, F.J.R.; Schwaiger, S.; Varela, R.M.; Molinillo, J.M.G.; Chinchilla, N.; Macías, F.A. Synthesis of Benzoxazinones Sulphur Analogs and Their Application as Bioherbicides: 1.4-Benzothiazinones and 1.4-Benzoxathianones for Weed Control. *Agronomy* **2023**, *13*, 1694. https://doi.org/10.3390/agronomy13071694

Academic Editors: Carolina G. Puig and Nuria Pedrol

Received: 23 May 2023
Revised: 22 June 2023
Accepted: 23 June 2023
Published: 25 June 2023

1. Introduction

Heterocyclic 1,4-benzoxazin-3-ones are interesting secondary metabolites produced by maize, wheat and rye. Cyclic hydroxamic acids are widely found in monocots, e.g., most plants in the Poaceae family, but also in the dicot clade such as the Acanthaceae, Ranunculaceae and Scrophulariaceae families [1]. The main relevant benzoxazinones are DIBOA (2.4-dihydroxy-2*H*-benzo[*b*][1,4]oxazin-3(4*H*)-one) and its methoxylated analog DIMBOA (2.4-dihydroxy-7-methoxy-2*H*-benzo[*b*][1,4]oxazin-3(4*H*)-one), which are found at high levels in young shoots of the aforementioned cereal crops. However, these compounds degrade to generate 2-amino-3*H*-phenoxazin-3-one (APO) and 2-amino-7-methoxy-3*H*-phenoxazin-3-one (AMPO), both of which have high phytotoxicity [2].

The latter compounds are of great interest from the point of view of allelopathy. APO and AMPO can prevent weed growth in species such as barnyardgrass (*Echinochloa crus-galli* L.) [3]. However, the difficulties in isolating this type of compound limit their field application. According to Copaja et al., an analysis of the tribe Triticeae showed that it is possible to obtain 20–5600 mg of DIBOA per kg of dried material and between 54.9–259.7 mg of DIMBOA per kg of dried plant [4]. Notwithstanding, the main active compound is the degradation product, and this further complicates the isolation of the potential bioherbicide.

A great deal of synthetic effort has been focused in recent years on obtaining larger quantities of these cyclic hydroxamic acids. Macías et al. studied benzoxazinone analogs to identify structure-activity relationships [5]. In addition, other non-natural derivatives have been prepared and examples include *N*-hydroxy-2-pyrrolidones [6] and (*S*)-2-hydroxy-1-oxo-1,2,3,4-tetrahydroisoquinoline-4-carboxylic acid [7]. These approaches allow us to generate a range of different derivatives to obtain a potent bioherbicide inspired by nature and control a wider variety of weeds by exploiting other mechanisms of action. At present, the most widely accepted mechanism for the disruption of weed growth is by inhibition of the function of histone acetyltransferases and histone deacetylases (HDAs) [8].

Sulfur analogs of the compounds discussed above have also been synthesized. Most examples are based on the replacement of the oxygen atom by sulfur (benzothiazinones) [9,10]. However, there are examples of different benzoxathianones in which the arrangement is based on a lactone instead of a lactam [11,12]. Kamila et al. developed a rapid methodology to synthesize alkyl derivatives in the α-position with respect to the carbonyl moiety by employing strong and uncommon bases [9]. Furthermore, Sicker et al. developed an efficient electrochemical synthesis that required different types of platinum catalyst [13].

The applications of the compounds discussed above have mainly centered on pharmacological uses such as anti-inflammatory, anti-tumor and anti-convulsant applications [13]. Despite the similarity of these analogs with benzoxazinones and their agricultural applications, the use of this sulfur scaffold in weed management has not been reported to date [14,15], although anti-aphid activity has been reported for the benzothiazinone moiety [16]. In the work described here, we propose a simple and economical synthesis method in which potassium hydroxide and methanol are employed to generate 1.4-benzothiazinone and 1.4-benzoxathianone derivatives from 2-aminothiophenol. In addition, in silico studies were conducted to evaluate the potential inhibition of HDAs and the values obtained were compared with those obtained in an in vitro bioassay against etiolated wheat coleoptiles and seeds of problematic weeds in crops of interest, such as *Echinochloa crus-galli*, *Lolium rigidum* and *Portulaca oleracea*.

2. Materials and Methods

2.1. General Experimental Procedures

2-Mercaptophenol, 2-aminothiophenol, ethyl bromoacetate, ethyl 3-bromopropionate, ethyl α-bromophenylacetate, acetyl chloride, ethyl 2-bromobutyrate and diethyl 2-bromo-2-methylmalonate were purchased from Aldrich Chemical Co. D-DIBOA and D-HBOA were prepared according to a literature procedure [17]. Ethyl acetate, *n*-hexane and chloroform (HiPerSolv Chromanorm® for HPLC) were obtained from VWR International (Radnor, PA, USA). The purities of all compounds were determined by NMR analyses. ^{1}H NMR, ^{1}H−^{1}H gCOSY, ^{1}H−^{13}C gHSQC and ^{1}H−^{13}C g-HMBC NMR spectra were recorded at room temperature using $CDCl_3$ as solvent on Agilent INOVA spectrometers at 400, 100 and 500, 125 MHz, respectively. The resonance of residual chloroform was set to δ 7.25 ppm for ^{1}H and to δ 77.0 ppm for ^{13}C. High-resolution mass spectra were recorded on a WATERS SYNAPT G2 mass spectrometer. Column chromatography was performed on silica gel (35−75 mesh) and TLC analysis was conducted using aluminium precoated silica gel plates.

2.2. Synthesis

2.2.1. General Methods for the Synthesis of 1.4-benzothiazinones and 1.4-benzoxathianone (1–6)

A 1 M solution of KOH in MeOH (100 mL) was added to a round-bottomed flask. A nitrogen atmosphere was applied and 2-aminothiophenol (1.25 g, 10 mmol) was added to the solution. The reaction mixture was stirred at room temperature and the color quickly changed from yellow to black (thiolate formation). Ethyl x-bromoalkyloate/aryloate (1.1 equiv) was added dropwise and the mixture was stirred overnight at room tem-

perature. Water (20 mL) was added and the MeOH was evaporated under reduced pressure (Figure 1). The product was extracted with ethyl acetate (3 × 20 mL) and the combined organic layers were dried (Na_2SO_4). The solvent was evaporated under reduced pressure and the crude product was purified by column chromatography (0–60% Hex:AcOEt).

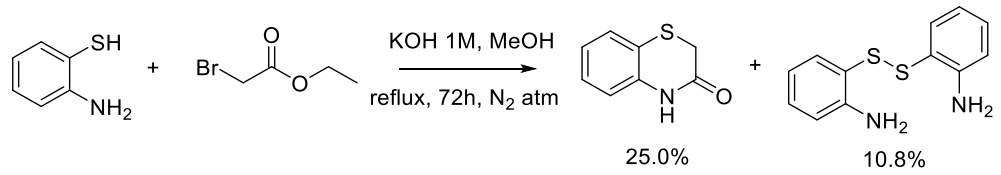

Figure 1. Reaction scheme for the formation of 1.

The synthetic method employed for this 1,4-benzoxathianone (**6**) was the same as that used for 1,4-benzothiazinones but using 2-hydroxythiophenol instead of 2-aminothiophenol. In this case the reaction mixture was heated under reflux.

Compounds 1–4 and 6 have been reported previously and the spectroscopic data and physicochemical properties are consistent with the target compounds (Figure 2). The ^{1}H and ^{13}C NMR data are presented as follows: (1, Supplementary Table S1, Figures S1 and S2), (2, Table S2, Figures S3 and S4), (3, Table S3, Figures S5 and S6), (4, Table S4, Figures S7 and S8), (5, Table S5, Figures S9 and S10), (6, Table S6, Figures S11 and S12). The yields obtained are as follows: (1, 25.0%), (2, 13.4%), (3, 30.6%), (4, 1,9%), (6, 6.1%). 2-Methoxy-2*H*-benzo[*b*][1,4]thiazin-3(4*H*)-one (5) was obtained as by-product during the cyclization reaction. The yield of this compound was 13.1%.

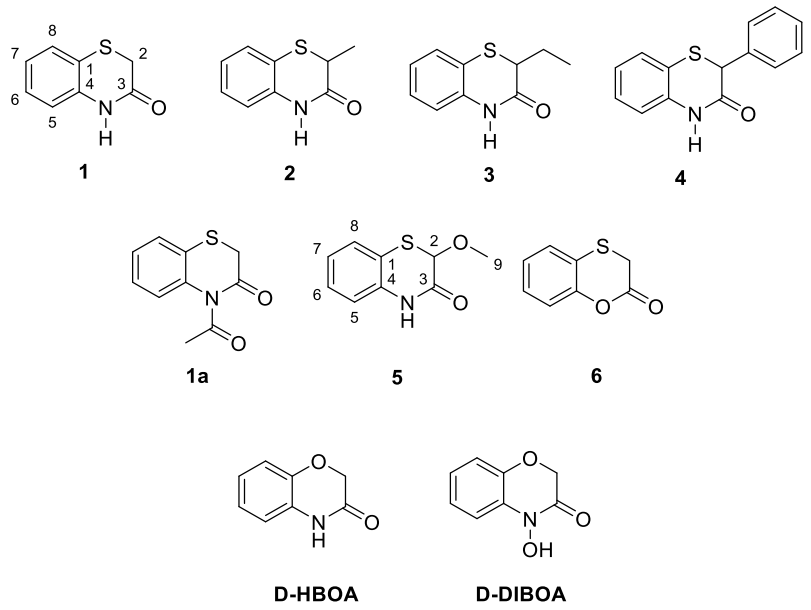

Figure 2. Structures of the 1.4-benzothiazinones and 1.4-benzoxathianones synthesized in this study and two 1.4-benzoxazinones.

2.2.2. Synthesis of 4-acetyl-2H-benzo[b][1,4]thiazin-3(4H)-one (1a)

Compound 1 (30 mg, 0.166 mmol) was dissolved in dry pyridine (1.5 mL) under argon. Acetyl chloride (2 equiv, 23.6 µL, 0.332 mmol) was added dropwise to the reaction mixture with stirring. The mixture was stirred at room temperature for 24 h. Water (10 mL) was added, and the product was extracted with ethyl acetate (3 × 10 mL). The combined organic extracts were washed with saturated aqueous $CuSO_4$ to remove pyridine and dried (Na_2SO_4). The solvent was removed under reduced pressure and the crude product was purified by column chromatography (0–80% Hex:AcOEt) to give a yellow oil (4 mg, $1.93 \cdot 10^{-2}$ mmol, 11.67% yield). HRMS: $C_{10}H_9NO_2S$ calculated: 207.0348 amu,

found $[M + Na]^+$: 230.0276 amu $[C_{10}H_8NO_2SNa]^+$. ^1H and ^{13}C NMR data are displayed in Table S7 and Figures S13 and S14.

2.3. In silico Experiments

2.3.1. Docking Experiments with HDA2 and HDA6

The 2D structures of the assayed compounds were generated with ChemBioDraw 20.0 (Perkin-Elmer Informatics Inc., Waltham, MA, USA) and were converted to 3D structures with GaussView 6.0.16 software (Gaussian, Inc., Wallingford, CT, USA). HDA6 protein was obtained from UniProt (https://www.uniprot.org/uniprot/Q9FML2-1, accessed on 16 February 2022). This protein (UniportCode: Q9FML2) is a prediction from AlphaFold® about HDAC groups in *Arabidopsis thaliana*, and it was a prediction based on 'histone deacetylases complex with peptide macrocycles' (6whn.1) with a 0.87 average model confidence. Low similarity in the predictions is located outside of the binding site. The software employed for docking was AutoDock® v.4.2. A grid box (60 × 60 × 60 Å) with a spacing of 0.425 Å was generated and centered on the Zn cofactor of the protein. Kollman charges were applied to each protein to simulate the electrostatic potential of amino acids. AutoDockTools (v. 1.5.6) was employed to define the previous steps. DFT B3LYP/6-311G(d,p) minimization was employed prior to conducting the docking. The Lamarckian GA algorithm with 20 GA runs was employed to develop the local docking, with a value of 1.0 used as the variance of the Cauchy distribution for gene mutations. All calculations correspond to the most populated cluster, with at least three members that fulfill an RMSD tolerance below 2.000 Å. Discovery Studio Visualizer 19.0 was used for the representation of the docking results.

2.3.2. Molecular Dynamics Experiments with HDA

Studies were conducted starting from the minimum energy protein-ligand conformation obtained from the molecular docking studies. GROMACS (2022.2 version) was employed in conjunction with the GROMOS54A7_atb force-field and the SPCE water model [18]. The ligand topologies and parameters were obtained using the SwissParam server (www.swissparam.ch). A dodecahedral box was generated, and the protein-ligand complex was at least 1 nm from the edges of the box, with a distance of at least 2 nm between periodic images of the protein to fulfill the minimum image convention. The zinc atom was constrained to the position specified by the X-ray crystallographic data reported. A 0.1 M NaCl concentration was simulated in the system to mimic physiological conditions. An energy minimization was applied until the maximum force was less than 10 kJ/mol. The system was then equilibrated for 0.1 ns with 2 fs per step at 300 K using canonical equilibration. Equilibration of the pressure was then conducted by the isothermal–isobaric method using the Parrinello–Rahman barostat. The system was equilibrated for 0.1 ns, also with 2 fs per step, at 300 K. The fully equilibrated system was submitted to a molecular dynamics simulation for 50 ns with 2 fs per step. Correction of the trajectory was conducted by protein recentering within the dodecahedral box. RMSD values were evaluated to analyze the kinetic of the protein-ligand complex generated and the ligand-zinc coordination kinetic. Ligand-protein and ligand-zinc energies were also evaluated for a quantification of the interaction. The average number of hydrogen bonds and average distance of these bonds were calculated using a 0.35 nm cut-off distance.

2.4. In Vitro Experiments

2.4.1. Etiolated Wheat Coleoptile Bioassay

Wheat seeds of *Triticum aestivum* L. cv. Burgos were sown in 15 cm diameter Petri dishes that were moistened with water. The seeds were then grown in the dark at a temperature of 25 ± 1 °C for a period of 4 days. After the shoots had grown, the roots and caryopses were removed. The top 2.0 mm of the latter were cut off using a van der Weij guillotine and discarded. The adjacent 4.0 mm sections of the coleoptiles were utilized for

the bioassay. In order to prevent further growth, all manipulations were conducted under a green safelight [19].

The compounds were dissolved in DMSO and then diluted in a phosphate/citrate buffer solution containing 2% sucrose at a pH of 5.6. This dilution was conducted to obtain consistent final concentrations for the assays (1000, 300, 100, 30 and 10 µM) with a consistent 0.1% DMSO content. Standard commercial herbicides such as Logran® (active ingredients 59.4% terbutryn and 0.6% triasulfuron), pendimethalin and Stomp® Aqua (active ingredient 45.5% pendimethalin) were also prepared in different solutions at the same concentrations for use as positive control samples. As a negative control, a solution of 0.1% DMSO in the phosphate/citrate buffer was also prepared.

To conduct the bioassay, 2.0 mL of either the test compounds, the positive control samples or the negative control samples were added to test tubes. Five coleoptiles with a length of 4.0 mm were placed in each test tube. Three replicates were conducted for each dilution. The tubes were then rotated at 0.25 rpm for 24 h at 25 ± 1 °C in the dark using a tube roller. After this period, the length of the coleoptiles was measured digitally using Photomed® 1.0 software and the statistical evaluation was conducted using Welch's test. The results are expressed as percentage differences from the negative control, so that positive values represent stimulation, while negative values indicate the level of inhibition achieved against the elongation of the coleoptiles.

2.4.2. Phytotoxicity Bioassay

The bioassays for *Echinochloa crus-galli*, *Portulaca oleracea*, and *Lolium rigidum* were conducted according to the method reported by Mejías et al. [20] with some modifications. The weed species used as target plants in this bioassay included the monocotyledons barnyard grass (*E. crus-galli* L.) and annual ryegrass (*L. rigidum* Gaud), and the dicotyledon common purslane (*P. oleracea* L.). The seeds for all three species were purchased from (Cantueso Natural Seeds Córdoba, Spain). Bioassays were conducted in Petri dishes (50 mm diameter) with one sheet of Whatman no. 1 filter paper. Germination and growth were conducted in aqueous solutions at controlled pH using 10^{-2} M 2-[*N*-morpholino] ethanesulfonic acid and 1 M NaOH (pH 6.0). The compounds to be tested were dissolved in a buffer and test concentrations of 1000, 300, 100, 30 and 10 µM were prepared. Prior to evaluating the standard dilutions, 0.5% *v*/*v* of dimethyl sulfoxide (DMSO) was added to enhance the solubility. Parallel controls were also run as described previously for etiolated coleoptile bioassays, but only pendimethalin was used as a positive control. Four replicates containing 20 seeds each were used. Treatment, control or internal reference solution (1 mL) was added to each Petri dish. The Petri dishes were sealed with Parafilm to ensure closed-system models. Seeds were incubated at 25 °C in a Memmert ICE 700 controlled environment growth chamber, with 24 h of darkness for all weeds. The bioassays took 8 days for each weed species, as reported previously [21]. After growth, plants were frozen at −10 °C for 24 h to prevent further growth during the measurement process. The parameters evaluated, including germination rate, root length and shoot length, were recorded using a Fitomed® v4.0 system, which allowed automatic data acquisition and statistical analysis using the associated software. Data were statistically analyzed using Welch's test, with significance fixed at 0.01 and 0.05. The results are presented as percentage differences with respect to the control, where zero represents control, positive values represent stimulation and negative values represent inhibition. The inhibition activity was calculated according to Equation (1), where *T* represents the treatment mean and *B* the blank mean (root/stem length or number of germinated seeds):

$$\text{Activity (\%)} = (\text{T} - \text{B})/\text{B} \times 100 \quad (1)$$

3. Results and Discussion

Benzoxazinoid scaffolds are very important from an allelochemical point of view, and we employed the same synthetic methodology as reported for the natural compounds by

Macías et al. [3]. The first step was the deprotonation of 2-aminothiophenol with KOH in MeOH under argon with heating under reflux. A color change from pale yellow to dark purple and then black was observed after a few minutes. Ethyl bromoacetate was added dropwise to the reaction mixture once the thiolate had formed. The mixture was stirred and heated overnight, and water was then added to stop the reaction. The MeOH was evaporated and EtOAc was then added in order to conduct a liquid–liquid extraction.

Purification of the crude product by column chromatography gave two different compounds. Firstly, 2.2′-disulfanediyldianiline was obtained in 0.86% yield. This compound was probably generated as a by-product at the beginning of the reaction due to the presence of a small amount of oxygen in the flask. The second compound obtained was the cyclized 1,4-benzothiazinone (**1**) and it is worth noting that the linear product was not obtained. It appears that after deprotonation of sulfur and the addition of ethyl 2-bromoacetate, nucleophilic attack on the carbonyl group by the amine begins. The yield of 2*H*-benzo[*b*][1,4]thiazin-3(4*H*)-one (**1**) is quite low (~3%). Most of the starting material did not react, but 2-aminobenzenesulfinic acid was observed along with a significant amount of 3*H*-benzo[*d*][1–3]dithiazole. These two compounds were probably generated after the addition of water in the work-up process and self-reaction, respectively. This initial approach was limited by the reaction time, and it was envisaged that the use of a prolonged reaction time could improve the yield.

The optimum reaction time was 72 h, after which the target compound was obtained in 25% yield. However, the production of 2.2′-disulfanediyldianiline upon prolonged reaction was not proportional to reaction time although it was higher than in the first approach. This observation led us to consider the conversion of 2.2′-disulfanediyldianiline after continuous exposure to the reactants. Experiments to evaluate the possible transformation of 2.2′-disulfanediyldianiline were conducted by following the same procedure as for 1.4-benzothiazinones but using this disulfide as the main reactant. It was found that after a reaction time of 24 h, there was no evidence for the formation of the proposed product. This finding indicates that the proposed reaction cannot occur after the formation of the by-product is complete.

Several derivatives at C-2 were synthesized in order to conduct QSAR studies (Figure 2). The use of ethyl 3-bromopropionate, ethyl 2-bromobutyrate, α-bromophenylacetate, propionyl chloride and acetyl chloride gave compounds 2, 3, 4, 5 and 1a, respectively. The NMR data show how the nature of the substituent leads to changes in the chemical shift of proton H-2, which is strongly deshielded at 4.92 ppm (i.e., +1.50 ppm) when the methoxy group is present in the molecule. Phenyl substitution also led to an increase in the chemical shift (4.70 ppm, i.e., +1.26 ppm) but this difference was less marked on analyzing the ^{13}C NMR spectrum (46.3 ppm, +16.4 ppm) in comparison with 5 (79.7 ppm, +49.8 ppm). In the case of compound 1a, the chemical shift of H-2 is the same (3.45 ppm, +0.01 ppm), but C-2 is deshielded to 36.0 ppm (+6.1 ppm). In addition, the longer the side chain, the higher the chemical shift of proton H-2. Optical rotation measurements were conducted to confirm the non-stereoselective reaction path. The optical rotation value was close to zero for all derivatives. As an example, compound 3 gave a rotation value of –0.35 ± 0.85° while theoretical +25 °C $[\alpha]_D$ values at the B3LYP/aug-cc-pVDZ level for (*R*)-3 and (*S*)-3 are –214.53 ± 14.22° and –200.66 ± 12.94°, respectively. So, no stereoselectivity is observed.

Literature methods for the synthesis of 1.4-benzothiazinones and 1.4-benzoxathianones involve electrochemical reduction of 2-nitrothiophenol derivatives [22,23] or microwave irradiation in the presence of an organic catalyst such as DBU [9]. In the case of compound 6, strong bases have been employed for the substitution of the generated thioacetamides toward the final 1.4-benzothiazinones [12,24]. However, we are able to obtain the expected compounds with inexpensive solvents and standard bases.

The reaction with diethyl 2-bromo-2-methylmalonate was conducted in order to introduce different functional groups in position C-2. It was expected that a methyl 3-oxo-3.4-dihydro or an ethyl 3-oxo-3.4-dihydro derivative would be obtained, but the Rutkauskas–Beresnevicius reaction occurred to generate a seven-membered ring. The

proposed reaction for the incorporation of the extra –CH_2– in the 1.4-benzothiazinones is provided in Figure 3. The ^{13}C-NMR signal was observed at 56.6 ppm and the C-2 position is deshielded to 48.2 ppm due to the substitution of the 2-aminothiophenol. ^{1}H NMR data also show two new protons in the aliphatic region, and these are geminal protons on the basis of the coupling constant (J = 16.8 Hz). HMBC experiments showed a connection between H-2a and H-2b with C-1 as well as C-1′. This information provides the link between the second aromatic ring and 1,4-benzothiazinones. Substitution of the 2-aminothiophenol could occur through the sulfur atom, but HMBC data show a connection with C-1′ (140.4 ppm), which can only be explained by an arrangement through the nitrogen. The singlet multiplicity of the methyl signals proves the nucleophilic substitution of the bromo-substituent by 2-aminothiophenol. The loss of the keto group close to the sulfur atom is explained by the significant production of 2.2′-disulfanediyldianiline during the reaction. The presence of a basic medium promotes the generation 2-aminobenzenethiolate and the new Rutkauskas–Beresnevicius product would act as a catalyst for the production of 2.2′-disulfanediyldianiline, which is reduced to obtain the –CH_2– observed in the NMR spectrum. The NMR and MS data that confirm the structure of the Rutkauskas–Beresnevicius product are provided in Table S8 and Figures S15–S17.

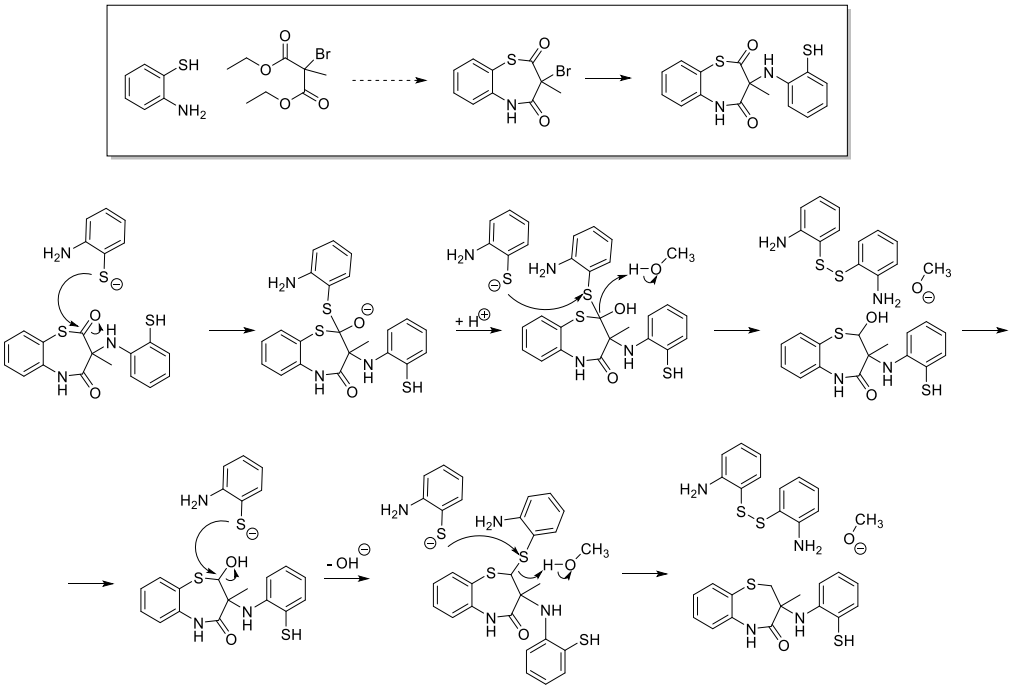

Figure 3. Reaction mechanism proposed for the product obtained in the reaction of 2-aminothiophenol and diethyl 2-bromo-2-methylmalonate.

Benzoxazinone mimics (compounds 1–6 and 1a) were evaluated in the etiolated wheat coleoptile bioassay along with synthetic derivatives D-DIBOA and D-HBOA to assess how the inclusion of the sulfur atom instead of oxygen affects the elongation of plant cells from wheat coleoptiles. The results for five different concentrations of the compounds are shown in Figure 4 along with those for three positive controls with different targets and formulations. Pendimethalin is a synthetic compound whose mode of action concerns plant cell division and elongation. Stomp® Aqua is the formulated version of pendimethalin and Logran® is a formulation of triasulfuron, which affects the biosynthesis of amino acids.

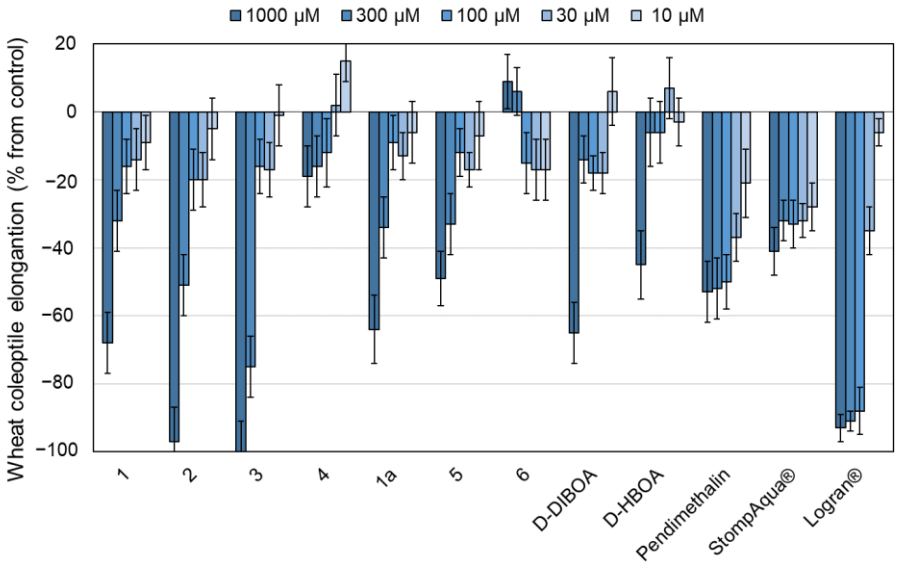

Figure 4. Wheat coleoptile bioassay results for 1.4-benzothiazinones and 1.4-benzoxathianones. Negative values represent inhibition of the elongation vs. control. Numerical data available in Table S9.

On considering compounds 2 and 3, it can be observed that at 1000 µM the inhibition is higher than that of the positive control Logran®. In the cases of pendimethalin and Stomp® Aqua, which are optimized to eliminate weeds and prevent side effects on wheat, there is limited inhibition of wheat coleoptile elongation, as one would expect. Compared with oxygen derivatives D-DIBOA and D-HBOA, the general phytotoxicity of S-D-HBOAs are better. For example, compound 1 and D-HBOA only differ by one atom (sulfur instead of oxygen) and the inhibition of the elongation is between 20% and 30% higher at 1000 µM and 333 µM, as can be deduced by comparing their corresponding IC_{50} values (Table S9). All of the derivatives, except for compounds 4, 5, and 6, show better IC_{50} values than the oxygen-containing derivatives. The derivative with the best profile is compound 3 showing an IC_{50} value of 211.1 µM (R^2 = 0.9551).

It is apparent that the substituents exert a clear effect and the presence of aliphatic chains at position C-2 leads to stronger inhibition of the plant cell elongation. However, the introduction of EDGs, such as phenyl rings or a methoxy group, decreases the phytotoxicity. On considering compound 6, it appears that the amide scaffold is one of the more relevant motifs to achieve activity. Acetylation at the *N*- position, e.g., compound 1a, does not affect the bioactivity much. This could be explained by fragmentation of the acetyl group and recovery of the full amide group to give compound 1. Indeed, the phytotoxicity profiles of these two compounds are rather similar and this supports the proposal outlined above.

In Vitro investigations were conducted to evaluate and understand the action of these compounds. Specifically, benzoxazinones and aminophenoxazines have been described as HDA inhibitors, so we hypothesized that these compounds could show similar modes of action through these targets. HDA6 was selected as a representative target for the protein family, and it was also employed for the biological studies of these natural products in previously published research. D-DIBOA, D-HBOA, compound 1 and compound 3 were evaluated by molecular docking to estimate the free energy of binding (ΔG) and the calculated inhibition constant (K_i). The values of both parameters were similar for all compounds evaluated, albeit with a slightly lower ΔG value for D-DIBOA (–3.03 ± 0.40 kcal/mol). This finding is consistent with previously reported results by Venturelli et al. [8], who demonstrated that the efficacy of 1.4-benzoxazinones is due to its oxidation products, aminophenoxazinones, which are more efficient in coordinating the zinc cofactor of HDAs. However, the replacement of oxygen by sulfur significantly modifies the charge distribution in the molecule. The Mulliken charges for all atoms in the main molecules studied are provided in Table S10 and it can be seen that the sulfur

atom holds a positive Mulliken charge while the oxygen in D-DIBOA and D-HBOA has a negative charge. Furthermore, there is a large transfer of charge toward the C-2 position, the negative Mulliken charge of which is doubled when D-DIBOA and 1 are compared. On examining the results obtained at the DFT B3LYP/LanL2DZ level, it can be seen that the Mulliken charge at C-2 has a higher negative value than those held by the oxygen atoms in D-DIBOA and D-HBOA. This fact influences the interaction of the zinc atom in HDA6 with the tested compounds. A direct interaction of this C-2 position with the zinc, instead of the sulfur atom, can be observed in Figure 5 and the situation with D-HBOA is expected to be similar.

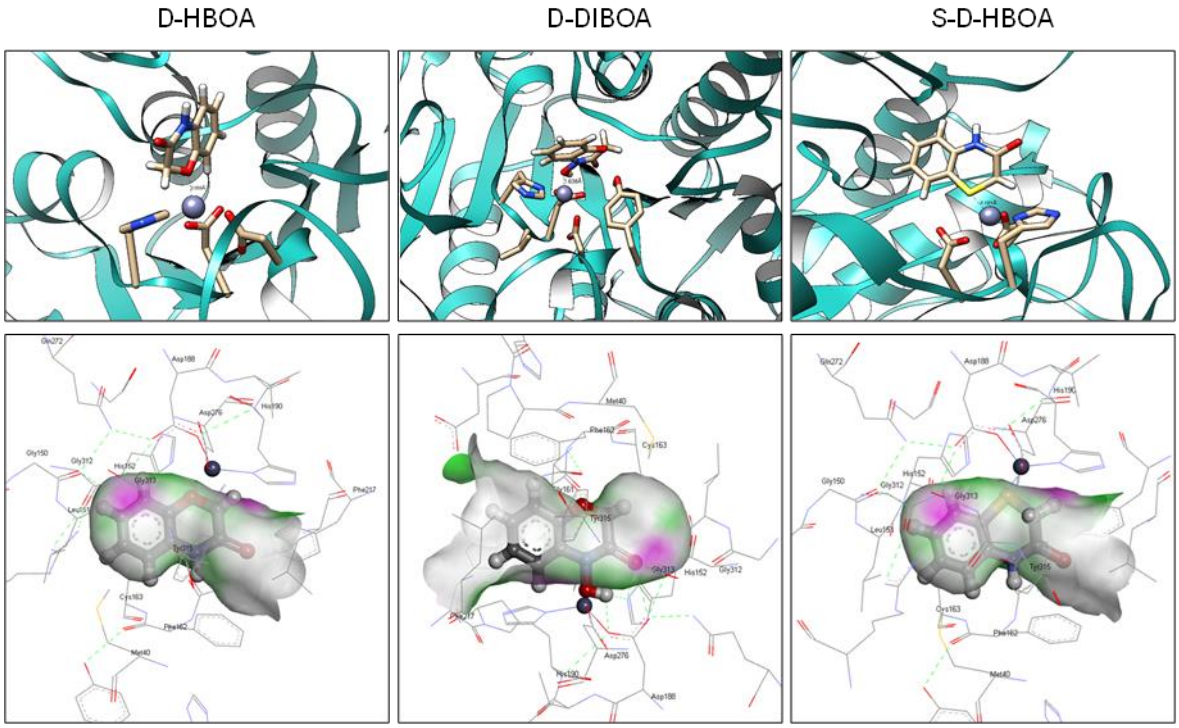

Figure 5. In silico docking of D-HBOA, D-DIBOA and S-D-HBOA (**1**) with HDA6 and donor-acceptor map of the ligands at the binding site. The pink color represents the donor position and the green color the acceptor positions.

The donor-acceptor map of the ligands at the binding site of HDA6 is shown in Figure 5 and this confirms the potential of the donor C-2 position to interact with the cofactor and the main residues involved in the coordination of the metal core.

In an effort to confirm the inhibition of HDA6, an in silico molecular dynamics analysis was performed to evaluate the stability of the inhibition complex with time, temperature and pressure. The simulation was performed along 50 ns and it shows the parameters related to the interaction between the ligands, the main protein and the zinc cofactor. Analysis of the root mean square deviation (Figure S18) indicates that the main arrangement observed by molecular docking was the most stable one. All of the ligands present rather small fluctuations, with variations of ±2 nm, and this shows a stable location at the site of action of the protein for the ligand [25]. In the case of D-HBOA, fluctuations are more marked up until the final part of the simulation. In contrast, compound **1** presents the lowest fluctuations with respect to the protein. However, on examining snapshots of the simulation it can be observed that the main interaction with the zinc cofactor is affected to a reasonable extent in terms of distance, complexation and energy.

It can be seen from Figure S19 that D-DIBOA does not change its location with respect to the protein site of action, but an interaction with zinc is not observed. For example, snapshots at 30, 40 and 50 ns do not show any interaction at all with the cofactor. Figure S20 reinforces this finding, and the interaction energy between zinc and D-DIBOA is almost

null. The results of this simulation have been confirmed experimentally by the mode of action reported by Venturelli et al. The chemical explanation for this lack of interaction is the same as that observed in the molecular docking and the DFT b3lyp/lanl2dz study, i.e., the negative Mulliken charges on the oxygen of the carbonyl group and the nitrogen are too low for complexation to the metal core to occur.

Interestingly, the interaction energy between D-HBOA and the zinc cofactor is very positive and shows a repulsive effect rather than inhibition of the protein by complexation with the metal. An RMSD study and the large number of hydrogen bonds with HDA6 seem to indicate good inhibition of the histone. However, the most important factor in the deactivation of the protein, namely the zinc atom, is not affected significantly by this compound (Figures S21). Compound 1 is the only example that displays a negative free interaction energy, and this suggests complexation of the zinc. This would explain why the presence of the sulfur atom instead of oxygen in compound 1 leads to higher phytotoxicity on the wheat coleoptile. Furthermore, this activity is again directly linked with the charge distribution in 1, with higher negative Mulliken charges for C-2, *O*-carbonyl and *N* positions. It can be observed in Figure 6 that the zinc atom is able to interact strongly with 1 due to intermolecular forces with the positions described above.

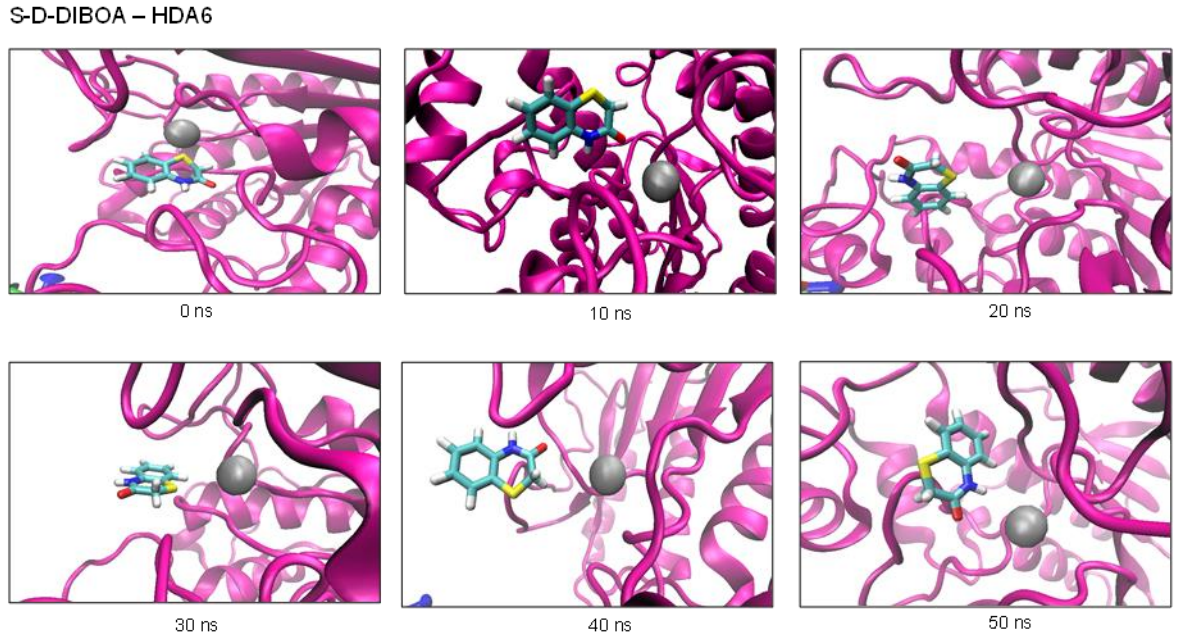

Figure 6. Snapshots of the molecular dynamic in silico simulation between HDA6 protein, D-DIBOA and zinc cofactor.

More specific bioassays that focus on weeds that infect rice [3], wheat [21,26] and barley [27] have been conducted. *Echinochloa crus-galli* (barnyard grass), *Lolium rigidum* (annual ryegrass), and *Portulaca oleracea* (common purslane) were evaluated at 1000, 333, 100, 33, and 10 µM with the most promising compounds (1, 2, 3, 1a, and 5) based on the results observed on etiolated wheat coleoptiles (Figure 4). The parameters studied in this assay were germination rate as well as root and shoot length. The results are represented in Figure 7. It can be clearly observed that germination mainly remains unaffected by the compounds. In the cases of the monocots, i.e., barnyard grass and annual ryegrass, the presence of an aliphatic chain as a substituent at position C-2 decreases the germination at a concentration of 1000 µM.

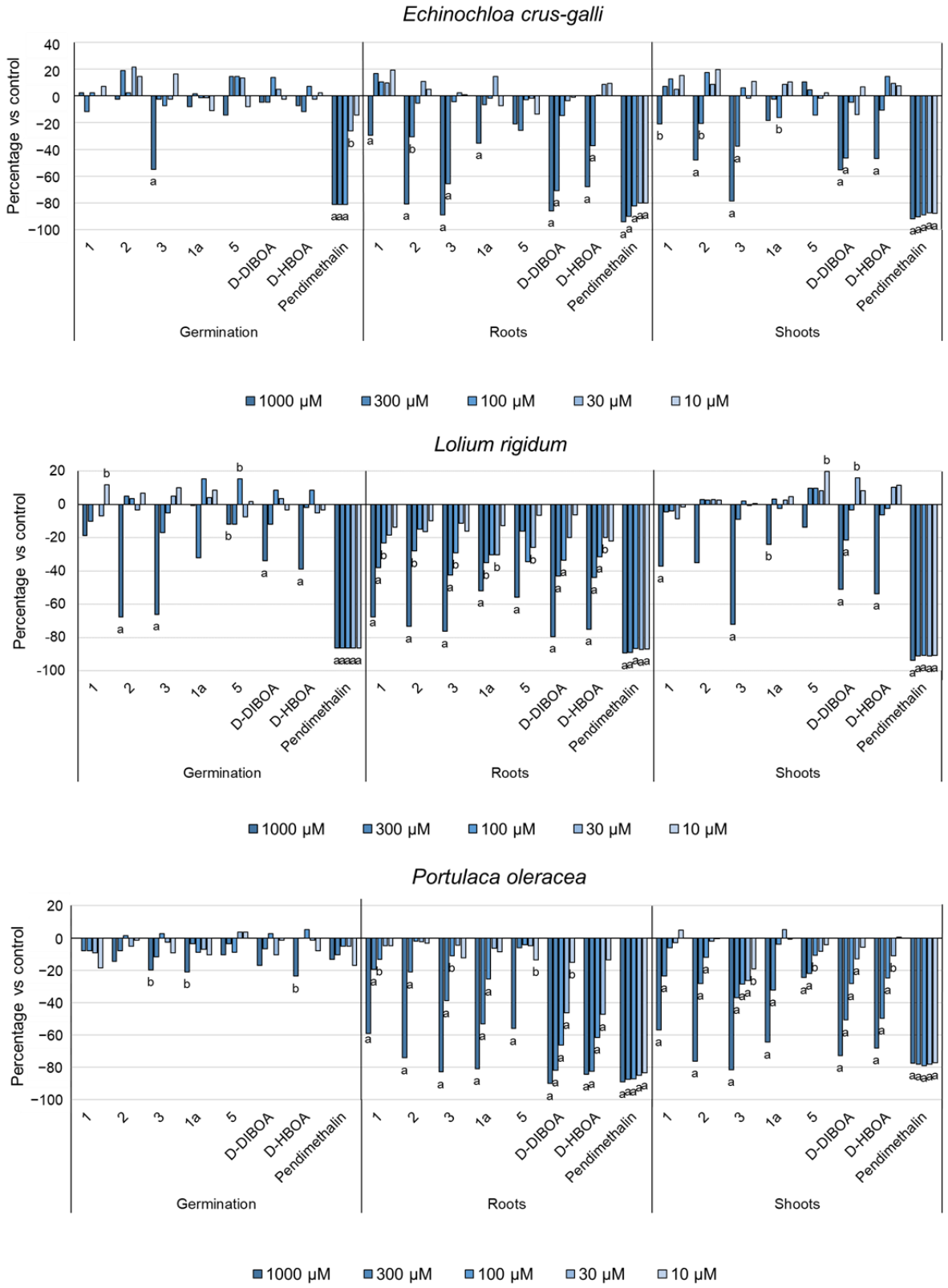

Figure 7. Results of the phytotoxicity study of S-D-HBOAs and benzoxazinones against *Echinochloa crus-galli*, *Lolium rigidum*, and *Portulaca oleracea*. Negative values represent inhibition in comparison with the control. Pendimethalin is the positive control. Values are expressed as the percent difference from the control. Significance levels $p < 0.01$ (a) or $0.01 < p < 0.05$ (b). There are letters a and b on the graph under the bars. It means the significance levels of our study. Numerical data available in Tables S11–S19.

The results also indicate that root formation is hardly affected after the addition of the S-D-HBOAs. In terms of the substituent, an aliphatic group, i.e., methyl or ethyl group, enhances the inhibition in all cases and it seems that the absence of a substituent on the nitrogen of the amide group is also advantageous in retaining activity. Compounds 2 and 3 display inhibition values similar to that of the positive control pendimethalin at 1000 and 333 μM for all of the weeds. Specifically, the IC_{50} values against barnyard grass and annual ryegrass are similar to those of D-DIBOA and D-HBOA (Table S11–S16). These benzoxazinones also show interesting values for all weed species studied. In the case of monocots, the activities of benzoxazinones are rather similar to those of compounds with sulfur, but they are more potent than the sulfur derivatives against eudicot (Table S17–S19). This behavior is different, however, on evaluating shoot inhibition and it can be observed that S-D-HBOAS presents higher values than benzoxazinones regardless of the clade, although the inhibition is more marked in eudicots (common purslane). This difference between roots and shoots for compounds 2 and 3 could be attributed to HDA action, which is more involved in the regulation of *de novo* shoot generation and formation rather than root control. According to Ma et al. and Temman et al., roots are also affected by HDA action, but their effects are more focused on root epidermis formation and hair induction than elongation or generation [28,29].

4. Conclusions

A general overview of the application of 1.4-benzothiazinones and 1.4-benzoxathianones for in vitro weed control is presented. Eight different compounds inspired by benzoxazinones were synthesized in one simple step with easy purification. These compounds have a sulfur atom instead of the oxygen atom present in benzoxazinones. Furthermore, a new derivative obtained by a Rutkauskas–Beresnevicius reaction was synthesized, and this allows the generation of new derivatives with applications in agriculture. These compounds were evaluated in vitro to assess their phytotoxicity in plant cells by the elongation of wheat coleoptiles. It was observed that the sulfur-containing compounds had higher inhibition than benzoxazinones and the positive control, especially at higher concentrations (1000 and 300 μM). Benzoxazinones have been described as histidine deacetylase inhibitors and the effects of 1.4-benzothiazinones and 1.4-benzoxathianones against HDA6, one of the most important enzymes of the family, were evaluated in silico by molecular docking and molecular dynamics. Docking results illustrated that the binding site of S-D-HBOAS is the same as that described previously for benzoxazinones, i.e., by chelation of the Zn cofactor. Furthermore, molecular dynamics experiments showed that the introduction of a sulfur atom instead of an oxygen leads to a rearrangement of the charges in the molecule, thus creating stronger interactions for the inhibition of HDA6. In vitro studies against *Echinochloa crus-galli*, *Lolium rigidum*, and *Portulaca oleracea* weeds gave interesting results against the growth of the roots for both monocots and dicots. Specifically, the inhibition is more pronounced against dicots, as in the case of common purslane, and the inhibition at a concentration of 1000 μM is similar to that of the classical herbicide employed as a positive control. In addition, for dicots the shoot growth is also affected, and higher inhibition is obtained when aliphatic groups are present in the C2 position of 1.4-benzothiazinones.

Supplementary Materials: The following supporting information can be downloaded at https://www.mdpi.com/article/10.3390/agronomy13071694/s1: Figure S1–S16: NMR spectra of compounds; Figure S17: LC-MS data of compounds. Figure S18: Root mean square deviation of the ligands respect to HDA6 protein and distribution and number of hydrogen; Figure S19: Snapshots of the molecular dynamic in silico simulation among HDA6 protein, D-DIBOA and zinc cofactor; Figure S20: Energy values between the ligands and zinc cofactor along the simulated molecular dynamic; Figure S21: Snapshots of the molecular dynamic in silico simulation among HDA6 protein, D-HBOA and zinc cofactor; Tables S1–S8: NMR data of compounds 1–6, 1a; Table S9: Phytotoxic values on coleoptile bioassay; Table S10: Mulliken charges distribution per atom. Table S11–S19: Phytotoxic values on weed bioassays.

Author Contributions: Conceptualization, F.J.R.M. and N.C.; methodology, F.J.R.M., R.M.V., N.C., J.M.G.M., S.S. and F.A.M.; software, F.J.R.M. and S.S.; validation, N.C. and F.J.R.M.; formal analysis, F.J.R.M. and J.M.G.M.; investigation, F.J.R.M., N.C., R.M.V., J.M.G.M., S.S. and F.A.M.; resources, F.J.R.M.; data curation, F.J.R.M.; writing—original draft preparation, F.J.R.M. and N.C.; writing—review and editing, F.J.R.M. and N.C.; visualization, N.C. and F.J.R.M.; supervision, F.A.M. and N.C.; Project administration, R.M.V. and F.A.M.; Funding acquisition, R.M.V., J.M.G.M. and F.A.M. All authors have read and agreed to the published version of the manuscript.

Funding: This work was financially supported by the Spanish Agencia Estatal de Investigación, grant number (PID2020-115747RB-I00) and the Andalusian Plan for Research, Development and Innovation (PAIDI 2020), grant number (ProyExcel_00860).

Institutional Review Board Statement: Not applicable.

Informed Consent Statement: Not applicable.

Data Availability Statement: Not applicable.

Acknowledgments: F.J.R.M. acknowledges the University of Cádiz—for postdoctoral support with a Margarita-Salas fellowship, funded by the European Union (NextGenerationEU)—and the University of Innsbruck for offering their facilities. A special acknowledgement is extended to the NMR Division from the Central Research Services for Science and Technology (SC-ICYT) of the University of Cadiz for the collaboration throughout the analysis of the samples.

Conflicts of Interest: The authors declare no conflict of interest.

References

1. Friebe, A. Role of Benzoxazinones in Cereals. *J. Crop. Prod.* **2008**, *4*, 379–400. [CrossRef]
2. Macías, F.A.; Oliveros-Bastidas, A.; Marín, D.; Chinchilla, N.; Castellano, D.; Molinillo, J.M.G. Evidence for an Allelopathic Interaction between Rye and Wild Oats. *J. Agric. Food Chem.* **2014**, *62*, 9450–9457. [CrossRef] [PubMed]
3. Macías, F.A.; Chinchilla, N.; Varela, R.M.; Molinillo, J.M.G.; Marín, D.; De Siqueira, J.M. Modified Benzoxazinones in the System *Oryza sativa-Echinochloa crus-galli*: An Approach To the Development of Biorational Herbicide Models. *J. Agric. Food Chem.* **2008**, *56*, 9941–9948. [CrossRef]
4. Copaja, S.V.; Barria, B.N.; Niemeyer, H.M. Hydroxamic Acid Content of Perennial Triticeae. *Phytochemistry* **1991**, *30*, 1531–1534. [CrossRef]
5. Macías, F.A.; Marín, D.; Oliveros-Bastidas, A.; Castellano, D.; Simonet, A.M.; Molinillo, J.M.G. Structure-Activity Relationships (SAR) Studies of Benzoxazinones, Their Degradation Products and Analogues. Phytotoxicity on Standard Target Species (STS). *J. Agric. Food Chem.* **2005**, *53*, 538–548. [CrossRef]
6. Yin, J.; Straub, M.R.; Liao, J.D.; Birman, V.B. Acylative Kinetic Resolution of Cyclic Hydroxamic Acids. *Org. Lett.* **2022**, *24*, 1546–1549. [CrossRef] [PubMed]
7. Bakulina, O.; Bannykh, A.; Dar'in, D.; Krasavin, M. Cyclic Hydroxamic Acid Analogues of Bacterial Siderophores as Iron-Complexing Agents Prepared through the Castagnoli-Cushman Reaction of Unprotected Oximes. *Chemistry* **2017**, *23*, 17667–17673. [CrossRef] [PubMed]
8. Venturelli, S.; Belz, R.G.; Kämper, A.; Berger, A.; von Horn, K.; Wegner, A.; Böcker, A.; Zabulon, G.; Langenecker, T.; Kohlbacher, O.; et al. Plants Release Precursors of Histone Deacetylase Inhibitors to Suppress Growth of Competitors. *Plant. Cell.* **2015**, *27*, 3175–3189. [CrossRef]
9. Kamila, S.; Koh, B.; Khan, O.; Zhang, H.; Biehl, E.R. Regioselective One Pot Synthesis of 2-Alkyl/Aryl-4h-Benzo[1,4] Thiazine-3-One via Microwave Irradiation. *J. Heterocycl. Chem.* **2006**, *43*, 1641–1646. [CrossRef]
10. Rutkauskas, K.; Beresnevicius, Z.I. Reaction of 2-Aminothiophenol with Acrylic Acid and Conversion of the Resultant Adducts. *Chem. Heterocycl. Compd.* **2006**, *42*, 227–232. [CrossRef]
11. Sakanashi, T.; Inagi, S.; Fuchigami, T. Highly Regioselective Anodic Monofluorination of 3H-1,4-Benzoxathian-2-Ones in Et4NF·4HF/MeCN. *Electrochemistry* **2008**, *76*, 896–899. [CrossRef]
12. Greenwood, D.; Stevenson, H.A. Benz-1:3-Oxathioles, Benz-1:4-Oxathien, and Aw-Bisarylthioalkanes. *J. Chem. Soc.* **1953**, *1*, 1514. [CrossRef]
13. Rathore, B.S.; Kumar, M. Design and Synthesis of 4H-1,4-Benzothiazines Containing Thiazole Ring System for Use as Potential Biopharmaceuticals. *Res. Chem. Intermed.* **2006**, *32*, 647–651. [CrossRef]
14. Chinchilla, N.; Marín, D.; Oliveros-Bastidas, A.; Molinillo, J.M.G.; Macías, F.A. Soil Biodegradation of a Benzoxazinone Analog Proposed as a Natural Products-Based Herbicide. *Plant. Soil.* **2015**, *393*, 207–214. [CrossRef]
15. Macías, F.A.; Chinchilla, N.; Arroyo, E.; Varela, R.M.; Molinillo, J.M.G.; Marín, D. Multifunctionalised Benzoxazinones in the Systems *Oryza sativa-Echinochloa crus-galli* and *Triticum aestivum-Avena fatua* as Natural-Product-Based Herbicide Leads. *Pest. Manag. Sci.* **2010**, *66*, 1137–1147. [CrossRef]

16. Escobar, C.A.; Sicker, D.; Niemeyer, H.M. Evaluation of DIMBOA Analogs as Antifeedants and Antibiotics towards the Aphid Sitobion Avenae in Artificial Diets. *J. Chem. Ecol.* **1999**, *25*, 1543–1554. [CrossRef]
17. Macías, F.A.; Marín, D.; Oliveros-Bastidas, A.; Chinchilla, D.; Simonet, A.M.; Molinillo, J.M.G. Isolation and Synthesis of Allelochemicals from Gramineae: Benzoxazinones and Related Compounds. *J. Agric. Food Chem.* **2006**, *54*, 991–1000. [CrossRef] [PubMed]
18. Schmid, N.; Eichenberger, A.P.; Choutko, A.; Riniker, S.; Winger, M.; Mark, A.E.; Van Gunsteren, W.F. Definition and Testing of the GROMOS Force-Field Versions 54A7 and 54B7. *Eur. Biophys. J.* **2011**, *40*, 843–856. [CrossRef] [PubMed]
19. Cárdenas, D.M.; Rial, C.; Varela, R.M.; Molinillo, J.M.G.; MacÍas, F.A. Synthesis of Pertyolides A, B, and C: A Synthetic Procedure to C17-Sesquiterpenoids and a Study of Their Phytotoxic Activity. *J. Nat. Prod.* **2021**, *84*, 2295–2302. [CrossRef]
20. Mejías, F.J.R.; Fernández, I.P.; Rial, C.; Varela, R.M.; Molinillo, J.M.G.; Calvino, J.J.; Trasobares, S.; Macías, F.A. Encapsulation of *Cynara cardunculus* Guaiane-Type Lactones in Fully Organic Nanotubes Enhances Their Phytotoxic Properties. *J. Agric. Food Chem.* **2022**, *70*, 3644–3653. [CrossRef]
21. Mejías, F.J.R.; Carrasco, Á.; Durán, A.G.; Molinillo, J.M.G.; Macías, F.A.; Chinchilla, N. On the Formulation of Disulfide Herbicides Based on Aminophenoxazinones: Polymeric Nanoparticle Formulation and Cyclodextrin Complexation to Combat Crop Yield Losses. *Pest. Manag. Sci.* **2023**, *79*, 1547–1556. [CrossRef]
22. Sicker, D.; Hartenstein, H.; Mouats, C.; Hazard, R.; Tallec, A. Electrochemical Reduction of O-Nitrophenylthioacetic Derivatives. Production of 2H-1,4-Benzothiazines. *Electrochim. Acta* **1995**, *40*, 1669–1674. [CrossRef]
23. Konno, A.; Naito, W.; Fuchigami, T.; Peters, D.G.; Motevalli, M.; Murase, H.; Shono, T.; Toftlund, H. Electrolytic Partial Fluorination of Organic Compounds. 33. Regioselective Anodic Monofluorination of Alpha-Phenylsulfenyl Lactams and Sulfur-Containing Nitrogen Heterocycles. *Acta Chem. Scand.* **1999**, *53*, 887–891. [CrossRef]
24. Pradhan, T.K.; Mukherjee, C.; Kamila, S.; De, A. Application of Directed Metalation in Synthesis. Part 6: A Novel Anionic Rearrangement under Directed Metalation Conditions Leading to Heteroannulation. *Tetrahedron* **2004**, *60*, 5215–5224. [CrossRef]
25. Mejías, F.J.R.; Durán, A.G.; Chinchilla, N.; Varela, R.M.; Álvarez, J.A.; Molinillo, J.M.G.; García-Cozar, F.; Macías, F.A. In Silico Evaluation of Sesquiterpenes and Benzoxazinoids Phytotoxins against M^{pro}, RNA Replicase and Spike Protein of SARS-CoV-2 by Molecular Dynamics. Inspired by Nature. *Toxins* **2022**, *14*, 599. [CrossRef]
26. Tabaglio, V.; Gavazzi, C.; Schulz, M.; Marocco, A. Alternative Weed Control Using the Allelopathic Effect of Natural Benzoxazinoids from Rye Mulch. *Agron. Sustain. Dev.* **2008**, *28*, 397–401. [CrossRef]
27. Macías, F.A.; Marín, D.; Oliveros-Bastidas, A.; Castellano, D.; Simonet, A.M.; Molinillo, J.M.G. Structure-Activity Relationship (SAR) Studies of Benzoxazinones, Their Degradation Products, and Analogues. Phytotoxicity on Problematic Weeds *Avena fatua* L. and *Lolium rigidum* Gaud. *J. Agric. Food Chem.* **2006**, *54*, 1040–1048. [CrossRef]
28. Temman, H.; Sakamoto, T.; Ueda, M.; Sugimoto, K.; Migihashi, M.; Yamamoto, K.; Tsujimoto-Inui, Y.; Sato, H.; Shibuta, M.K.; Nishino, N.; et al. Histone Deacetylation Regulates de Novo Shoot Regeneration. *PNAS Nexus* **2023**, *2*, pgad002. [CrossRef] [PubMed]
29. Ma, X.; Lv, S.; Zhang, C.; Yang, C. Histone Deacetylases and Their Functions in Plants. *Plant. Cell. Rep.* **2013**, *32*, 465–478. [CrossRef]